14th International Conference on Greenhouse Gas Control Technologies, GHGT-14

21st -25th October 2018, Melbourne, Australia

Efficient Liquefaction of Carbon Dioxide on Superomniphobic Surfaces

Ingrid Snustad[a], Åsmund Ervik[b], Anders Austegard[b], Gunhild Reigstad[b], Jianying He[a], Zhiliang Zhang[a], Amy Brunsvold[b,*]

[a]*Norwegian University of Science and Technology, Trondheim, Norway*
[b]*SINTEF Energy Research, Trondhiem, Norway*

Abstract

Liquefaction of CO_2 is a necessary step in several parts of the carbon capture, transport and storage (CCS) chain, e.g. for processing for ship transport. By increasing the efficiency of condensation, a lower energy consumption is achieved and hence, costs are reduced for CCS. Increased condensation efficiency can be achieved by inducing dropwise condensation instead of the conventional filmwise condensation. This switch in condensation mode is caused by alterations of the surface on which the condensation occurs and can be achieved by structuring the surface on the nanoscale and coating with low surface energy chemicals.
In this work we have built a new experimental setup to investigate the condensation process. The setup consists of a highly instrumented pressure chamber that can operate up to 25 bar with a high purity CO_2 atmosphere, and a condensation surface that can be cooled to -55ºC. Visual observation is performed through a sight glass in the pressure vessel using a high-speed camera. The process of CO_2 condensation is visually monitored and the contact angle, contact angle hysteresis, and mode of condensation on different surfaces can be found.
Keywords: CCS; efficient condensation; CO_2 liquefaction; engineered surfaces

Nomenclature

CCS	Carbon capture, transport and storage

1. Introduction

To reduce anthropogenic CO_2 emissions, large-scale carbon capture, transport and storage (CCS) must be deployed worldwide [1]. A major barrier to widely implemented CCS technologies are the high costs, mainly associated with the capture process, but also along the whole CCS chain. One key part of the chain is CO_2 condensation, which is a necessary process step e.g. for ship transportation. By increasing the liquefaction heat transfer rates, one can reduce the energy consumption, and effectively reducing the costs associated with the process.

Most gases will condense on a metal surface in the filmwise mode of condensation. The condensation process starts when a saturated gas forms liquid nuclei at specific nucleation sites, i.e. heterogeneous nucleation, followed by coalescing of the first droplets into a thin liquid film. Once the film is formed, the continued condensation follows the

* Corresponding author. Tel.: +47 930 02 419
E-mail address: amy.brunsvold@sintef.no

direct condensation path where the gas condenses directly into the film, i.e. homogeneous condensation. The liquid film acts as a thermal resistance between the cold condensing surface and the gas, hence the process is slowed down by the presence of the liquid film. This can be overcome by inducing dropwise condensation, for which the initial nuclei grow into droplets through direct condensation and coalescence. The droplets continue to grow and are eventually shed by gravity, due to the liquid-phobic nature of the surface. This leads to fresh nucleation sites on the surface and is therefore a more efficient mode of condensation.

Dropwise condensation was first described by Schmidt et al. [2] in 1930. Since then the phenomena have attracted significant attention in the research community as well as in industry. With dropwise condensation it is possible to achieve a heat transfer coefficient up to an order of magnitude higher than that of filmwise condensation [3-7]. For dropwise condensation to dominate the behaviour, the solid surface on which the condensation occurs must be manipulated to repel the condensate. A typical way is to construct a superomniphobic surface (for water, the surface is called superhydrophobic), which is a surface on which any liquid has a contact angle above 150º and a contact angle hysteresis below 10º. The adhesion between droplet and surface will be minimal, and the droplets easily roll of the surface after condensation. Since there is no film present to act as a thermal resistance towards heat transfer from gas to surface, the heat transfer efficiency is increased.

The design and creation of a superomniphobic surface is a complex process, though some successful reports of superphobic surfaces against low surface tension fluids exist [7-10]. Several design criteria for a superomniphobic surface have been suggested [11], but to realize the theoretical best surface could be very challenging, if not impossible for the liquids with very low surface tension. CO_2 is such a liquid, with a surface tension of 4mN/m at 0ºC [12]. For comparison, the surface tension of water is 72mN/m at 20ºC. For eventually achieving dropwise condensation of CO_2, more knowledge is needed about the condensation process on conventional flat metal surfaces.

This work consists of the design and construction of a completely new and innovative experimental setup for visual observation of the condensation process. It is built for CO_2 condensation, but is not limited to this one chemical component. The setup is therefore powerful in understanding condensation on a small scale and on different types of structured and flat surfaces of different materials. This work also presents preliminary results of the new knowledge that the setup can give. The condensation process of CO_2 on two different surfaces have been investigated. The surfaces are flat aluminium and a superhydrophobic aluminium surface.

2. Experimental

A new experimental setup has been designed and built especially for revealing the condensation process of CO_2. With the setup the temperature and pressure can be accurately controlled and measured while the condensation process progresses. The setup's main parts are the specially designed pressure chamber and a high-speed camera (Phantom Slow Motion V9.1). The pressure chamber is a stainless-steel tube with a 20 cm inner diameter and a length of 15 cm. The tube is closed off by two flanges in which one is a double flange with a see glass in the center. Through the wall of the tube there is inlet and outlet for the CO_2 atmosphere in the chamber, as well as inlet and outlet for the second CO_2 loop, which is used to cool the condensing surface. In addition, a sealed high-pressure feedthrough for the necessary electric wires is welded to the wall. There are wires for 3 thermocouples, 4 LED lights and a rotation motor through the feedthrough. The device is custom made for the purpose and consists of a 16 mm OD tube that is filled with two-component epoxy glue to support the inner pressure. In addition, each individual wire with insulation is closed off with the same epoxy to stop gas flow between wire and insulation. The pressure chamber and the feedthrough are designed for a working pressure of 25 bar.

To ensure that no vapor from air condenses on the lens of the camera or the see-glass into the chamber, the setup is lowered into a freezer (Scandomestic SB 650), and the air in the freezer is dried (Kaeser DC 4.2 PSA air dryer). The temperature in the freezer is about -13ºC and the relative humidity is 1-3%.

The crucial part of the setup is the condensing element which cools the condensing surface to the requested temperature, between -20ºC and-50ºC for pressures between 20 and 6 bar, respectively. The condensing element is a rectangular slab of copper, 4 cm x 5 cm wide and 1 cm high. The inside of the slab consists of narrow channels 0.4 mm wide and 0.5 mm apart, in which two-phase (liquid-gas) CO_2 flows at a predetermined and accurately controlled pressure. Initially in the cooling loop, liquid CO_2 is supplied by using a gas cylinder with a raiser pipeline at pressures above the liquid pressure at ambient temperature. Some of the liquid will then evaporate to let the pressure reach the

saturation pressure that is the setpoint of the cooling loop. The setpoint is controlled by an automatic back pressure regulator (Alicat Scientific PCR3). Two-phase flow is then achieved, and following the coexisting curve of gas and liquid, the temperature is accurately determined by the pressure. The temperature is measured at the inlet and at the outlet of the condensing element and a deviation of around 0.5K is observed. This is within the accuracy of the T-type thermocouples (Omega), and the temperature is assumed uniform throughout the condensing element.

Two 1 mm slits are carved into the surface of the condensing element. Two T-type thermocouples (Omega) are placed in the slits and attached with thermally conductive silver paste. The silver paste is homogeneously spread in the slits and on the copper surface and acts as a glue for the investigated surfaces. It is important to ensure that the paste is homogeneously spread and that there are no air bubbles. This is for ensuring that the heat flux is uniform in the vertical direction from the vapor to the condensing element across the entire surface. In this way the temperature measured directly underneath the surface is as close as possible to the actual condensing temperature.

During experiments, the pressure chamber is filled with pure CO_2 (Aga, grade 5.2). The pressure is controlled by an automatic dual-valve pressure regulator (Alicat Scientific PCD), placed at the inlet of the gas. The regulator keeps the pressure constant within 0.1 bar. The temperature in the chamber is measured by two thermocouples (Omega) placed directly above and below the condensing element. The temperature is determined by the temperature in the freezer and varies between -15°C and -10°C.

A far-field objective lens is mounted to the high-speed camera. At the highest speed of 1000 fps the maximum resolution is 1632x1200. Movies and snapshots are recorded by Phantom PCC software and analyzed with ImageJ.

Two different surfaces have been investigated; plain aluminum and a commercial superhydrophobic aluminum surface. The surfaces are illuminated with one, two or three LED lights (Cree XLamp). The LED's are placed one on each side and one directly above the surface, and the operator has freedom to choose whichever LED to use, or which combination to use, in order to achieve the best contrast. The condensation process is monitored at -30°C for the plain copper and commercial surface, while at -30°C and -50°C for the plain aluminum.

3. Results and discussion

The condensation on both surfaces follows the filmwise condensation mode, as expected, since none of the surfaces are designed and fabricated for condensation of low surface tension fluids. The condensation starts when the pressure in the chamber is slightly above the saturation pressure at the given temperature in the two-phase flow. This is expected as the temperature at the surface is influenced not only by the condensing element's internal temperature, but the temperature in the saturated gas and the fact that the adhesion between surface and cooper through the conductive paste is not perfect. The condensation starts at around 14.3 bar, at set temperature of -30ºC. The set-temperature is achieved within the heat exchanger, in the two-phase flow. The measured temperature in the surface (by the thermocouples in the slits), is 1-2ºC higher than the set temperature, and the pressure in the chamber is therefore higher than in the condensing element loop when the condensation occurs.

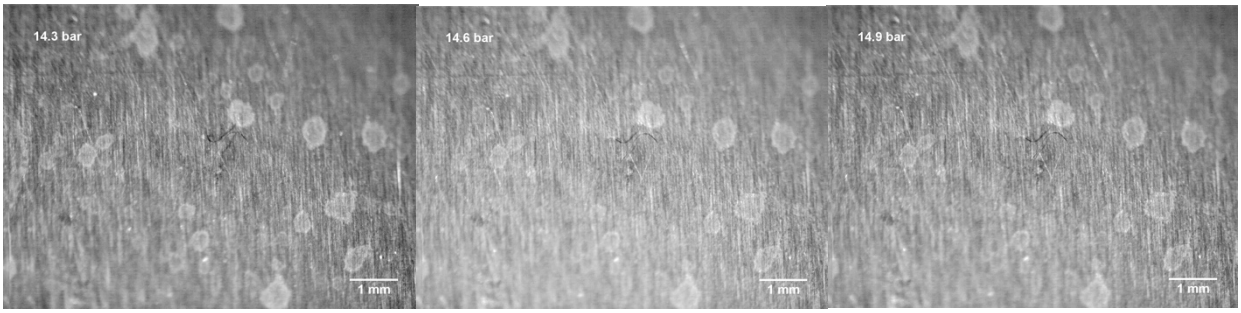

Figure 1 Plain aluminium surface at 14.3 bar (left), 14.6 bar (middle) and 14.9 bar (right). The surface appears darkest before condensation (14.3 bar) and becomes brighter as the surface is covered with a thin liquid film (14.6 bar). At 14.9 bar the surface again appears darker, as the film thickness increases.

Figure 1 shows the flat aluminum surface when the surface is slightly below, exactly at, and above the saturation pressure. The aluminum surface is macroscopically flat but has microscopic roughness. The roughness influences the nucleation step of the condensation, as the nucleation sites will be more or less likely to occur in a scratch or uneven area of the surface. Especially if the unevenness is caused by dust or other impurity laying on the surface. This can be seen in Figure 4.

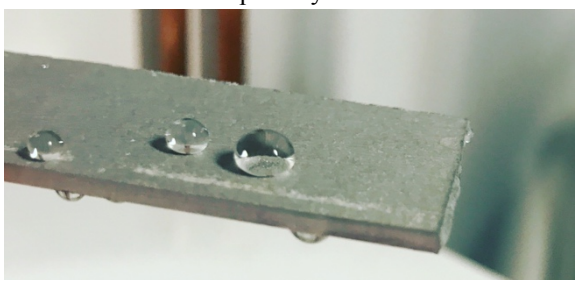

Figure 2 Water droplets on superhydrophobic aluminium surface

The second surface is a commercial superhydrophobic aluminum surface. Figure 2 shows how water is repelled from the surface. The surface is structured on the micro and macro scale and roughness is visible to the naked eye. No coating is used, so the surface consists solely of aluminum. CO_2 condenses in the filmwise mode on this surface as well, as is evident from Figure 3. The figure shows three snapshots of the condensation process, at 14.3, 14.4 and 14.6 bar. The condensation process is initiated between 14.3 and 14.4 bar and starts with condensation into small nuclei. This can be said with the basis in the difference in brightness in the two leftmost pictures. The lighter appearance of the surface at 14.4 bar results from many small droplets reflecting the light in all directions. When further increasing the pressure, the surface again appears dark, which is caused by the liquid film covering the surface, which is seen to the right in Figure 3.

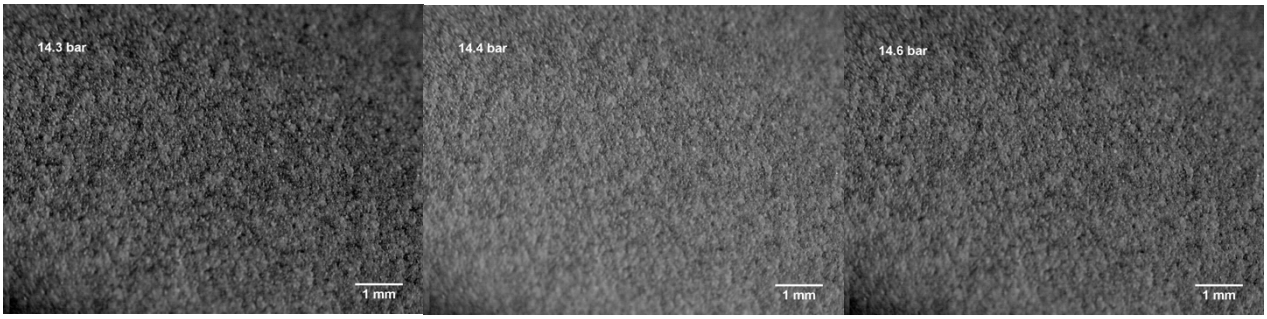

Figure 3 Superhydrophobic surface at 14.3 bar (left), 14.4 bar (middle), and 14.6 bar (right). The brighter appearance at 14.4 bar is caused by condensation of droplets and the spreading of light due to the droplets. The image at 14.6 bar is again darker due to the formation of a continuous liquid film.

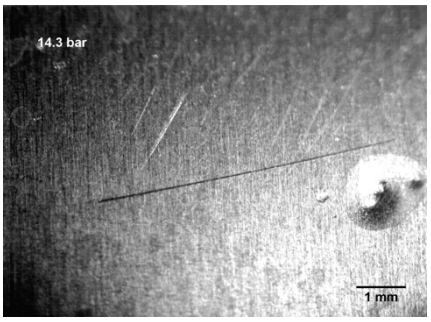

Figure 4 Liquid CO_2 trapped at dust particle on aluminium surface. Image is captured during evaporation.

4. Conclusion

A new experimental setup has been designed and build for qualitative characterization of CO2 condensation on various surfaces. The setup can be used from -50ºC to room temperature and a pressure range from 1 to 20 bar. The setup has been used for characterizing the condensation of CO_2 on flat and micro-nanostructured aluminum, which occurs in the filmwise mode.

Acknowledgements

This publication has been produced with the support of the Research Council of Norway through the CLIMIT funding program (254813/E20).

References

[1] International Energy Agency. Energy Technology Perspectives 2017. OECD Publishing; 2017.
[2] Schmidt, E, Schurig, W, Sellschopp, W. Versuche uber die Kondensation von Wasserdampf in Film- und Tropfenform. Technische Mechanik und Thermodynamik 1930; 1:2-p. 53
[3] Boreyko, JB, Chen, C-H. Self-Propelled Dropwise Condensate on Superhydrophobic Surfaces. Physical Review Letters 2009; 103:18-p. 184501
[4] Ma, X, Rose, JW, Xu, D, Lin, J, Wang, B. Advances in dropwise condensation heat transfer: Chinese research. Chemical Engineering Journal 2000; 78:2-3-p. 87
[5] Sikarwar, BS, Battoo, NK, Khandekar, S, Muralidhar, K. Dropwise Condensation Underneath Chemically Textured Surfaces: Simulation and Experiments. Journal of Heat Transfer 2010; 133:2-p. 021501
[6] Weisensee, PB, Neelakantan, NK, Suslick, KS, Jacobi, AM, King, WP. Impact of air and water vapor environments on the hydrophobicity of surfaces. Journal of Colloid and Interface Science 2015; 453:177
[7] Preston, DJ, Lu, Z, Song, Y, Zhao, Y, Wilke, KL, Antao, DS, Louis, M, Wang, EN. Heat Transfer Enhancement During Water and Hydrocarbon Condensation on Lubricant Infused Surfaces. Scientific Reports 2018; 8:540-p.
[8] Kota, AK, Kwon, G, Tuteja, A. The design and applications of superomniphobic surfaces. NPG Asia Materials 2014; 6:7-p. 109
[9] Tuteja, A, Choi, W, Mabry, JM, McKinley, GH, Cohen, RE. Robust omniphobic surfaces. Proceedings of the National Academy of Sciences 2008; 105:47-p. 18200
[10] Wu, T, Suzuki, Y. Design, microfabrication and evaluation of robust high-performance superlyophobic surfaces. Sensors and Actuators B: Chemical 2011; 156:1-p. 401
[11] Snustad, I, Røe, IT, Brunsvold, A, Ervik, Å, He, J, Zhang, Z. A review on wetting and water condensation - Perspectives for {CO2} condensation. Advances in Surface and Interface Science 2018; 256:291
[12] Quinn, EL. The surface tension of liquid carbon dioxide. Journal of the American Chemical Society 1927; 49:11-p. 2704